Research Article

Hongcheng Zhou*

Design model-free adaptive PID controller based on lazy learning algorithm

https://doi.org/10.1515/jisys-2022-0279
received December 02, 2022; accepted June 23, 2023

Abstract: The nonlinear system is difficult to achieve the desired effect by using traditional proportional integral derivative (PID) or linear controller. First, this study presents an improved lazy learning algorithm based on k-vector nearest neighbors, which not only considers the matching of input and output data, but also considers the consistency of the model. Based on the optimization index of an additional penalty function, the optimal solution of the lazy learning is obtained by the iterative least-square method. Second, based on the improved lazy learning, an adaptive PID control algorithm is proposed. Finally, the control effect under the condition of complete data and incomplete data is compared by simulation experiment.

Keywords: lazy learning, search strategy, PID control algorithm, optimal solution

1 Introduction

With the development of information science and technology, the production process and manufacturing technique of enterprises are becoming more and more complex. In the practical engineering application, many examples have verified the effectiveness and practicability of proportional integral derivative (PID) control [1]. Scholars have proposed the robust adaptive backstepping control strategy based on the wavelet neural network [2]. The common algorithms include offline reference trajectory-based guidance method, online trajectory-based guidance method, and prediction guidance method.

But the mechanism modeling or identification modeling of these processes faces enormous challenges. As a control method that does not require the precise model of the controlled object and only relies on the input/output (I/O) data and other control information of the control system to complete the control tasks of the system, data-driven control has gradually become the focus of modern control field research. The database selection rules that have impact on the data-driven control method are modified, including the size of the database capacity, the principle of data elimination and retention, so as to achieve efficient online update of data.

Because of the nonlinear system strong uncertainty, it is difficult to achieve the desired effect by using traditional PID or linear controller. With the development of control theory and technology, many adaptive control methods have been proposed. When using these advanced control methods, it is necessary to identify the control system model [3]. The online identification uses a rolling data window to identify the local model of the current running point. The offline identification requires the nonlinear model of the system, and then, the local linearization model of the system is obtained by the linearization of the working point. In the actual system control, these control methods have achieved good results. But it takes a lot of time and cost to obtain the reliable identification results, and the controller designed by this method becomes more complex with the change of the identification work point [4]. In this article, the PID method that can change the linearized model and update the control parameters adaptively according to the working point change was studied.

* **Corresponding author: Hongcheng Zhou,** School of Electronic and Information Engineering, Jinling Institute of Technology, Nanjing 211169, China, e-mail: zhouhcnj@163.com

2 Adaptive PID control based on lazy learning

2.1 An improved algorithm for lazy learning identification

The lazy learning algorithm is to find the similar data in the sample data and then use the best linear combination approximation of the basis function in the local model of the adjacent domain [5]. The local model is used to obtain the output data corresponding to any input data in the adjacent domain.

The production process and manufacturing technique are becoming more and more complex. And the mechanism modeling or identification modeling of these processes faces enormous challenges. As a control method that does not require the precise model of the controlled object and only relies on the I/O data and other control information of the control system to complete the control tasks of the system, data-driven control has gradually become the focus of modern control field research. In this study, the model-free adaptive PID control is based on the lazy learning algorithm.

For a class of the Single input single output systems, the discrete model expression is as follows [6]:

$$y(i) = f_1(y(i-1), \cdots, y(i-n_y), u(i-p), \cdots, u(i-p-n_u)) + \varepsilon(i), \tag{1}$$

where $y(\cdot)$ is the system output, $u(\cdot)$ is the control input, n_y is the system output order, n_u is the system input order, $p > 0$ is the time delay of the system input and output, $f(\cdot)$ is the unknown function of the system dynamic, and $\varepsilon(i)$ is the white noise interference signal.

The aforementioned expression can be transformed into the following expression:
$y_i = f_1(X_i) + \varepsilon_i$, where $X_i = [y(i-1), \cdots, y(i-n_y), u(i-p), \cdots, u(i-p-n_u)]^T$.

In this study, we consider an unknown multi-input single-output nonlinear mapping $f_1(X_i) : R^n \to R$ and assume measurable I/O data: $\{(X_i, y_i)\}_{i=1}^N$, where $X_i \in R^n$ and $y_i \in R$. The random variable $\varepsilon_i \in R$ satisfies the independent random distribution in which the mean value is 0 and the variance is σ^2.

In accordance with the basic identification principle, the identification problem based on the lazy learning algorithm obtains the corresponding relations of I/O data under the given sample set and further gives any given vector X_q, and the output estimate $\hat{y}_q$ is given by using the corresponding relation [7,8]. Therefore, it can be summarized as the following optimization problem:

$$\min \sum_{(X_i, y_i) \in \Omega_k} (y_i - f_1(X_i, \theta))^2 w_i, \tag{2}$$

where Ω_k is the local space of the nearest X_q, k samples; $f_1(\cdot)$ is the nonlinear mapping function of I/O vector; and w_i is the degree to which the input data of the local space affects the output data. That is, the nearest input value corresponding to the input vector distance can reflect the current output vector.

The mathematical expression for an input vector X_q with k samples in local space Ω_k is as follows:

$$\Omega_k \triangleq \{X_1, X_2, \cdots, X_k\} = \{X_i | d(X_i, X_q) < h\}, \tag{3}$$

where $h \in R$ is the radius of the neighborhood space Ω_k, which determines the number of samples in the input vector neighborhood space, as a distance function $d(\cdot)$, to measure the distance between the samples and to determine whether the samples are in the current neighborhood space Ω_k. In this case, if there are k samples in a neighborhood space Ω_k, then these samples are recorded as $X_1, X_2, \cdots, X_k$. For a domain Ω_k, any value in the domain is taken as an input data, and then the output data of the object model can be estimated by the value under the input using the identified mapping function $\hat{f}_1(\cdot)$ [9,10].

At the input vector X_q, the system-related local functional expression $f(.,.)$ can be expressed as a p-th-order polynomial expression:

$$\hat{f}_1(\mathbf{X}, \theta) = \theta_0 + \theta_1(\mathbf{X}_i - \mathbf{X}) + \cdots + \theta_p(\mathbf{X}_i - \mathbf{X})^p = \theta^T \varphi_i, \tag{4}$$

where $\theta = [\theta_0, \theta_1, \cdots, \theta_p]^T$; $\varphi_i = [(X_i - X_q)^0, (X_i - X_q)^1, \ldots, (X_i - X_q)^P]$; then, the optimization problem for (2) can be expressed as:

$$\theta = \arg\min_{\theta_j} \sum_{i=1}^{k} \left\{ y_i - \sum_{j=0}^{p} \theta_j (X_i - X_q)^j \right\}^2 w_i. \tag{5}$$

In these expressions, the functional relationship w_i between the data window h and the distance $d(X_i,\ X_q)$, that is, $w_i = K\left(\frac{d(X_i,\ X_q)}{h}\right)$, the effect of the sample X_i on the local modeling of the system, is usually determined by the kernel function.

In this study, we consider not only the fitting accuracy of the input and output, but also the smoothness of the fitting model; the input and output pairs of the fitted model are guaranteed not to change dramatically at the adjacent sampling time. From (4), when the input data $\mathbf{X}_i$ is close to the current value $\mathbf{X}$, the corresponding output should be close, and the derivatives should be close to ensure the smoothness of the model [11,12]. And the optimization parameter is the parameter that represents each order derivative. Therefore, in order to guarantee the smoothness of the fitting model, it is reasonable to use some constraints on the optimization parameters θ as a penalty term [13]. In this study, the spherical constraint on the parameters θ is chosen as the penalty term, so that the solution of the model-fitting optimization problem can be expressed as follows: $\theta = \arg\min_{\theta_j}\left\{\sum_{i=1}^{k}[y_i - \sum_{j=0}^{p}\theta_j(X_i - X_q)^j]^2 w_i + \alpha_t\ \|\theta - \bar{\theta}\|^2\right\}$.

The aforementioned formula can be simplified as follows:
$\theta = \arg\min_{\theta_j}\left\{\sum_{i=1}^{k}[y_i - \varphi_i^T\theta]^2 w_i + \alpha_t\ \|\theta - \bar{\theta}\|^2\right\}$.

For this optimization problem, the iterative solution process is summarized as follows.

Theorem: *for performance index function*:

$$J_2(\theta) = \sum_{k=1}^{t} (y_k - \varphi_k^T\theta)^2 w_k + \alpha_t \|\theta - \bar{\theta}\|^2. \tag{6}$$

The penalty factor is

$$\alpha_t = \left(\log\left(\sum_{k=1}^{t} \|\varphi_{k-1}\|^2\right)\right)^{1+\delta},\quad \delta > 0. \tag{7}$$

The performance index is $J_2(\theta)$. The solution $\min_{\theta\in S(\bar{\theta},\varepsilon)} J_2(\theta)$ is in the following recursive form: $T_0 = P_{i-1},\ i = 1 \to n$. Set: $T_0 = P_{i-1},\ i = 1 \to n,\ \phi_i = \begin{bmatrix} 0 & \cdots & \underset{\substack{\uparrow \\ i}}{1} & \cdots & 0 \end{bmatrix}$.

The recursive expression is

$$T_i = T_{i-1} - \frac{(\alpha_t - \alpha_{t-1}) T_{i-1}\phi_i\phi_i^T w_i T_{i-1}}{1 + (\alpha_t - \alpha_{t-1})\phi_i^T T_{i-1}\phi_i w_i}, \tag{8}$$

$$P_t = T_n - \frac{T_n\varphi_{t-1}\varphi_{t-1}^T w_{t-1} T_n}{1 + \varphi_{t-1}^T T_n \varphi_{t-1} w_{t-1}}. \tag{9}$$

Thus, the recursive least-square estimate of the unknown parameter vector is the following:

$$\hat{\theta}_t = \hat{\theta}_{t-1} + P_t\varphi_{t-1}(y_t - \varphi_{t-1}^T\hat{\theta}_{t-1})w_{t-1} + P_t(\alpha_t - \alpha_{t-1})(\bar{\theta} - \hat{\theta}_{t-1}), \tag{10}$$

where

$$\begin{aligned} r_t &= r_{t-1} + \|\varphi_{t-1}\|^2 \\ \alpha_t &= (\log(r_t))^{1+\delta},\quad \delta > 0 \end{aligned} \tag{11}$$

Proof: Because the performance index $J_2(\theta)$ is quadratic form with respect to an unknown parameter θ, we obtain an estimated value of the parameter θ.

$$\hat{\theta}_t = \left[\sum_{k=1}^{t} \varphi_{k-1}\varphi_{k-1}^T w_{k-1} + \alpha_t I\right]^{-1} \cdot \left[\sum_{k=1}^{t} y_{k-1}\varphi_{k-1} w_{k-1} + \alpha_t \bar{\theta}\right]. \tag{12}$$

To obtain a recursive expression of the parameter estimated value $\hat{\theta}_t$, the matrix P_t is defined as follows:

$$P_t = \left[\sum_{k=1}^{t} \varphi_{k-1}\varphi_{k-1}^T w_{k-1} + \alpha_t I\right]^{-1}. \tag{13}$$

Thus, the estimated value $\hat{\theta}_t$ can be expressed as:

$$\hat{\theta}_t = P_t\left[\sum_{k=1}^{t} y_{k-1}\varphi_{k-1} w_{k-1} + \alpha_t \bar{\theta}\right], \tag{14}$$

$$\sum_{k=1}^{t} y_{k-1}\varphi_{k-1} w_{k-1} = y_{t-1}\varphi_{t-1} w_{t-1} + \sum_{k=1}^{t-1} y_{k-1}\varphi_{k-1} w_{k-1} = y_{t-1}\varphi_{t-1} w_{t-1} + P_{t-1}^{-1}\hat{\theta}_{t-1} - \alpha_t \bar{\theta}. \tag{15}$$

Substituting (15) into P_t^{-1} can yield:

$$P_t^{-1} = P_{t-1}^{-1} + \varphi_{t-1}\varphi_{t-1}^T w_{t-1} + (\alpha_t - \alpha_{t-1})I. \tag{16}$$

Substituting (15) into (14) can yield:

$$\begin{aligned}\hat{\theta}_t &= P_t\{y_{t-1}\varphi_{t-1}w_{t-1} + [P_t^{-1} - \varphi_{t-1}\varphi_{t-1}^T w_{t-1} - (\alpha_t - \alpha_{t-1})I]\hat{\theta}_{t-1} - \alpha_{t-1}\bar{\theta} + \alpha_t\bar{\theta}\} \\ &= \hat{\theta}_{t-1} + P_t\varphi_{t-1}(y_t - \varphi_{t-1}^T\hat{\theta}_{t-1})w_{t-1} + P_t(\alpha_t - \alpha_{t-1})(\bar{\theta} - \hat{\theta}_{t-1}).\end{aligned}$$

The aforementioned expression is (10) in theorem. For equation (16), the inverse operation is taken on both sides at the same time, and the matrix inverse lemma formula is used to obtain

$P_t = [P_{t-1}^{-1} + \varphi_{t-1}\varphi_{t-1}^T w_{t-1} + (\alpha_t - \alpha_{t-1})I]^{-1} =$

$[P_{t-1}^{-1} + (\alpha_t - \alpha_{t-1})I]^{-1} - [P_{t-1}^{-1} + (\alpha_t - \alpha_{t-1})I]^{-1} \frac{\varphi_{t-1}\varphi_{t-1}^T w_{t-1}}{1 + \varphi_{t-1}^T [P_{t-1}^{-1} + (\alpha_t - \alpha_{t-1})I]^{-1}\varphi_{t-1} w_{t-1}} [P_{t-1}^{-1} + (\alpha_t - \alpha_{t-1})I]^{-1}$.

The abbreviations are $T_n = [P_{t-1}^{-1} + (\alpha_t - \alpha_{t-1})I]^{-1}$.

P_t can be further abbreviated to $P_t = T_n - \frac{T_n\varphi_{t-1}\varphi_{t-1}^T w_{t-1} T_n}{1 + \varphi_{t-1}^T T_n \varphi_{t-1} w_{t-1}}$.

Thus, (19) in theorem is obtained, and (18) in theorem can be obtained inversely.

This theorem is consistent with the least-square estimation of the unknown parameter vectorθ. When the least-square solution is obtained, the autoregressive model estimation of the object can be obtained by substituting the model (14).

$$\hat{y}_i = \hat{f}_1(X_i, \ \theta). \tag{17}$$

In this way, the Jacobian information matrix of the object model can be obtained.

$$\frac{\partial y_i}{\partial u_i} \approx \frac{\partial \hat{y}_i}{\partial u_i}. \tag{18}$$

2.2 Design adaptive PID controller based on lazy learning

In the practice of PID control, because of the variety of control objects, the parameters of PID controller need to be adjusted repeatedly. Although there are only three parameters of PID controller, which correspond to the coefficients of proportional, differential, and integral, respectively; the linear combination of each parameter cannot guarantee the control effect if we want to obtain a good control effect [14,15]. In order to find the optimal combination from the almost infinite coefficient combination sequence, it is necessary to adopt the optimization method. Here, Jacobian matrix by the lazy learning algorithm can be used to optimize PID control parameters k_p, k_i, and k_d by adaptive optimization algorithm.

The design of the neural network adaptive PID controller based on the lazy learning is realized by the following two steps:

(1) First, the classical PID controller structure is given. The PID controller uses the output data and control instructions of the system to control the controlled object directly, and its three parameters k_p, k_i, and k_d will be selected in the next step.
(2) Then, a lazy learning algorithm is used to obtain the local model of the object, and Jacobian information of the controlled object at the current time is calculated. The optimal parameters of PID controller corresponding to some optimal index function are obtained by using the gradient principle.

The classical PID controller is expressed in an incremental form as:

$$u(t) = u(t-1) + k_p(e(t) - e(t-1)) + k_i e(t) + k_d(e(t) - 2e(t-1) + e(t-2)). \tag{19}$$

In the aforementioned expression, k_p, k_i, and k_d represent the proportional, integral, and differential coefficients, respectively.

The performance index function for the original continuous system is

$$\boldsymbol{E}(t) = \frac{1}{2}(r(t) - y(t))^2. \tag{20}$$

For the system of I/O data sampling and the object model estimation by the lazy learning algorithm, the parameters are set as follows:

$$E(k) = \frac{1}{2}e(k)^2 = \frac{1}{2}(r(k) - \hat{y}(k))^2. \tag{21}$$

Using the gradient descent to adjust the PID parameters k_p, k_i, k_d and using the identification result of the lazy learning algorithm, the following rules can be obtained [16]:

$$\begin{aligned}
\Delta k_p &= -\eta_p \frac{\partial E}{\partial k_p} = -\eta_p \frac{\partial E}{\partial u}\frac{\partial u}{\partial k_p} = \eta_p e(k)\frac{\partial \hat{y}}{\partial u}(e(k) - e(k-1)) \\
\Delta k_i &= -\eta_i \frac{\partial E}{\partial k_i} = -\eta_i \frac{\partial E}{\partial u}\frac{\partial u}{\partial k_i} = \eta_i e(k)\frac{\partial \hat{y}}{\partial u}e(k) \\
\Delta k_d &= -\eta_d \frac{\partial E}{\partial k_d} = -\eta_d \frac{\partial E}{\partial u}\frac{\partial u}{\partial k_d} = \eta_d e(k)\frac{\partial \hat{y}}{\partial u}(e(k) - 2e(k-1) + e(k-2)).
\end{aligned}$$

The structure of the adaptive PID controller based on the lazy learning algorithm is shown in Figure 1. The whole controller is composed of PID controller, lazy learning algorithm module, and adaptive mechanism module. In the lazy learning module, the object is modeled locally by the input and output sampled data of the object, and the parameters of the model change with the change of the system working state. The Jacobian

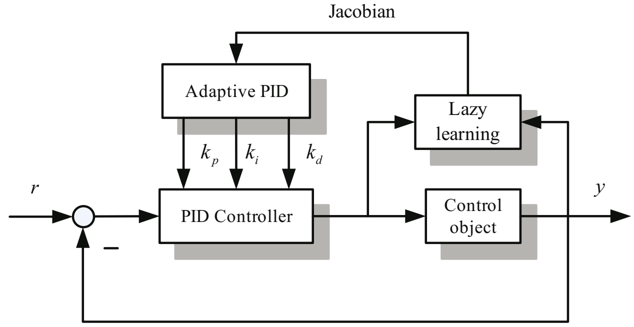

Figure 1: Structure of adaptive PID controller based on the lazy learning algorithm.

matrix of the controlled object is approximated by the local model, and then, the adaptive module uses the approximate value to optimize the PID parameters and gives its adaptive dynamics. In this way, a complete adaptive PID controller based on lazy learning can obtain the optimal solution of PID parameters in real time with the change of the working state of the controlled object, thus realizing model-free adaptive control.

3 Simulation

Continuous stirred tank reactor (CSTR) is an important part of chemical production [17]. It is a typical nonlinear object in chemical system. Its dynamic equation is

$$\begin{cases} \frac{\mathrm{d}C_a}{\mathrm{d}t} = \frac{q}{V}(C_{af} - C_a) - k_0 C_a \exp(-E/RT), \\ \frac{\mathrm{d}T}{\mathrm{d}t} = \frac{q}{V}(T_f - T) + \frac{(-\Delta H)k_0 C_a}{\rho C_p}\exp(-E/RT) + \frac{\rho_c C_{pc}}{Q_c C_p} Q_c\left[1 - \exp\left(\frac{-hA}{Q_c \rho_c C_{pc}}\right)\right](T_{cf} - T), \end{cases} \tag{22}$$

where C_a is the the concentration value of the product A in the reactor, T is the the temperature of the reactant, q is the flow rate of incoming and outgoing material, and Q_c is the flow rate of the coolant. According to the requirements of the modern technology, the concentration value C_a, reactant temperature T, control variable Q_c, and external disturbance variables T_c, q, and C_{af} are determined. The schematic diagram is shown in Figure 2 [18].

The input information vector of the system model is shown in the following:

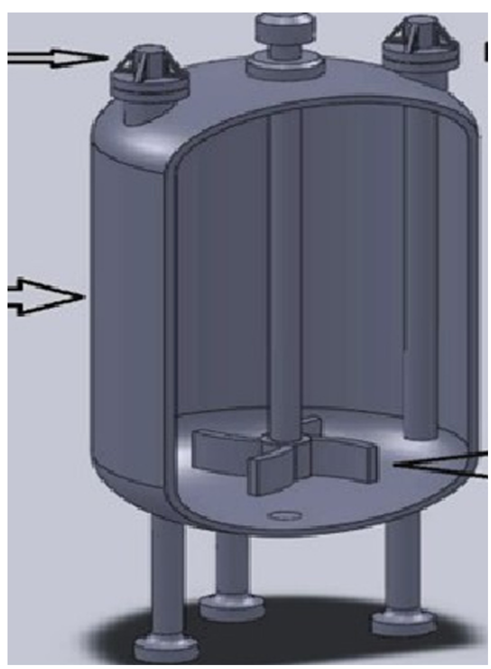

Figure 2: Schematic diagram of CSTR.

$$\phi(t-1) = [T(t-1),\ T(t-2),\ Q_c(t-1),\ Q_c(t-2)]. \tag{23}$$

The local model order is $n_y = 2$ and $n_u = 1$. The lazy learning online modeling parameters are $\alpha = 0.85$ and $k \in [12, 100]$. PID controller penalty term is $Q = 9.3$.

3.1 Simulation and verification of completeness data

Temperature T output tracking setting is $yr = (443 \rightarrow 447 \rightarrow 438.5)$.

Figure 3 shows that the lazy learning control algorithm can quickly track the modeling data when the running points of the system change. The system output can track the given output value without static error, and there is no overshoot. Under the third instruction, the system can track the given output value without static error, but the overshoot occurs, and its tracking speed is faster. This reflects the inherent contradiction between the overshoot and the tracking speed. The presence of overshoot is more apparent in Figure 3.

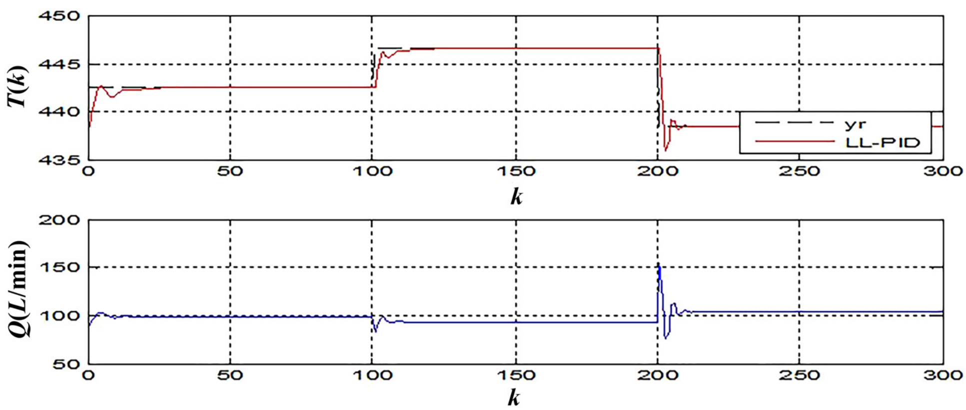

Figure 3: CSTR response curve.

In the whole tracking trajectory, the PID control parameters change as shown in Figure 4. As can be seen from the diagram, when the instruction changes from the first to the second, the parameter transformation of the controller is mainly reflected in the integral term, while when the instruction changes from the second to the third, the parameters of the controller vary greatly in all three components. This is also the reason why the dynamic performance of the control result changes greatly at this time. The simulation results show that the neural network PID control based on a real-time learning can realize the output tracking control of CSTR, and the control effect is good.

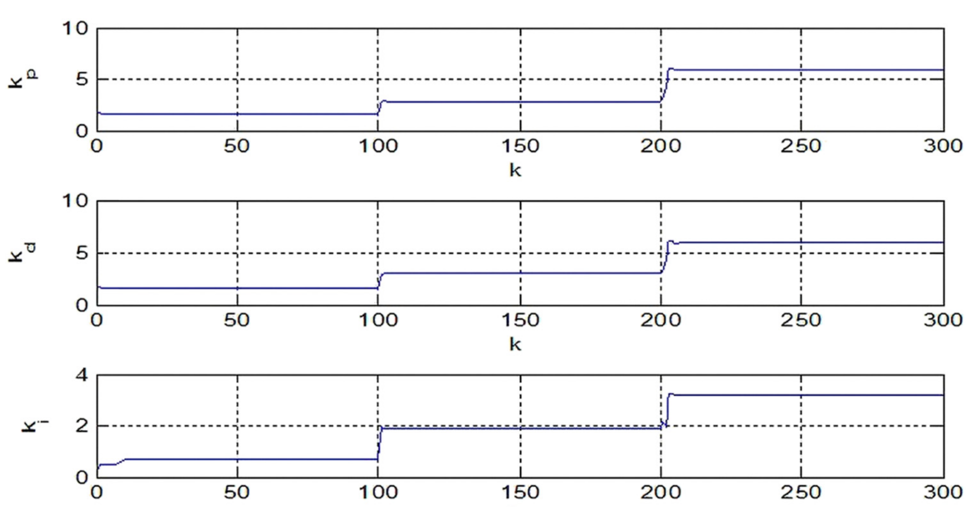

Figure 4: Variation curve of PID controller parameters.

3.2 Simulation and verification of incomplete data

Temperature T output tracking is $yr = (444 \rightarrow 451 \rightarrow 442)$.

The output tracking value of 451 is not in the working condition interval covered by the data, so the original 2,000 sets of samples are not complete under the new control goal, and now the closed loop control is carried out under these data; based on this, the stability of the closed-loop system is analyzed and the tracking performance is compared under the condition of complete data and incomplete data [19,20]. The controller parameter is selected as $c^T = [15 \quad 10]$. $q = 0.8$, $g = 0.95$, and $m = 0.01$. The simulation results are shown in Figures 5 and 6. Figure 5 is the parameter change curve of PID control. It can be seen that the tracking performance of the proposed algorithm depends more on the completeness of the data. If the training data cannot cover the whole working range completely, the tracking performance will be greatly reduced.

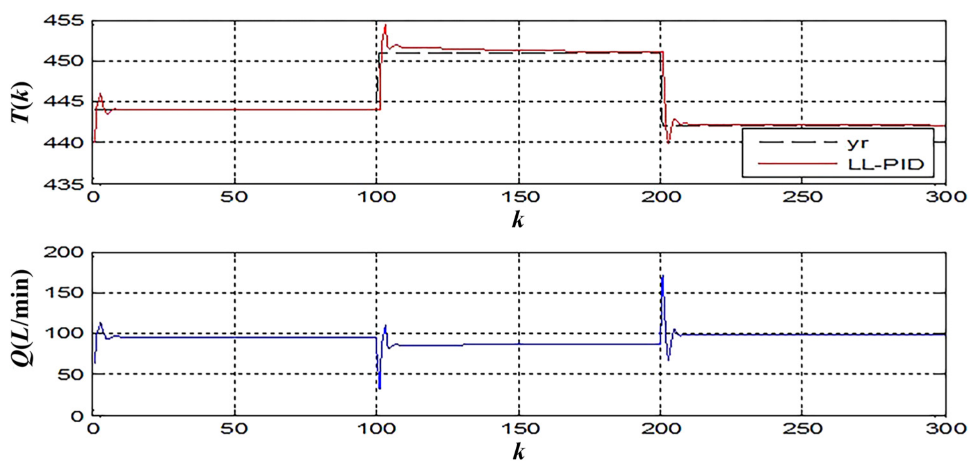

Figure 5: CSTR response curve (incomplete data).

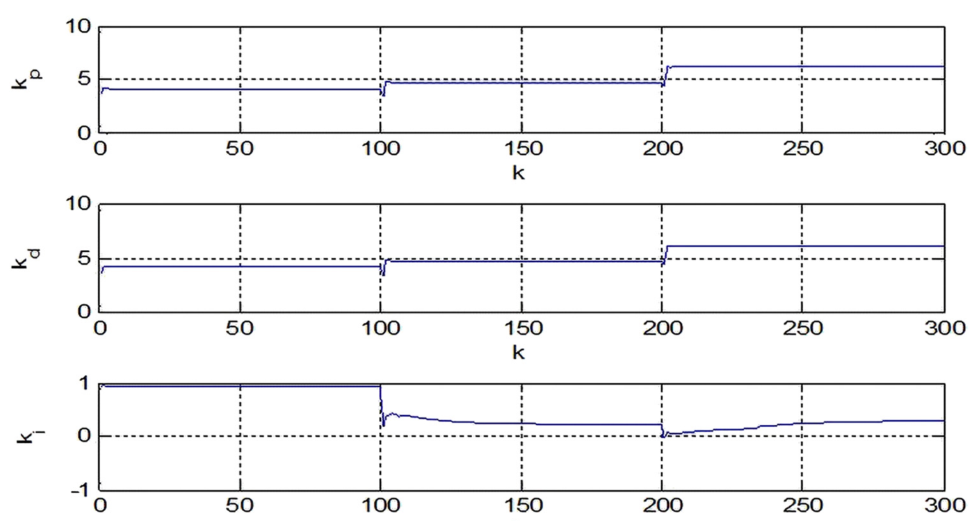

Figure 6: Variation curve of PID controller parameters (incomplete data).

As can be seen from Figure 5, the neural network PID method can adjust the temperature well when the control target is in the effective coverage of the data collected, such as when the temperature instruction is 444 and 442 K. But the control target is not in the coverage of the sampled data, for example, when the temperature instruction is 451 K, the control effect of neural network PID is not ideal, there is a large overshoot, and the steady-state error becomes smaller gradually. As can be seen from the diagram, the neural network can still realize the temperature control when the data is not perfect, but the control effect is not ideal.

Figure 6 shows the variation of the control parameters. It can be seen that the proportional and differential feedback parameters do not change much under various temperature commands, but the integral parameters do. This is in accordance with the engineering experience and the physical meaning of PID control. Because the temperature command is a trapezoid signal and the tracking speed and overshoot of the command are not important in the optimization index of control parameters, the selection of control parameters is mainly determined by the adjustment error of output. Therefore, the parameter that deals with the steady-state error changes more obviously in the control process; it is well known to PID control that this parameter is the integral feedback parameter. As can be seen from Figure 6, the magnitude of the variation of the integral parameter is the largest in the control process, and it is almost constant when the instruction parameter is not in the valid range of the sampled data.

The performance index of parameter updating was further optimized, and the control quantity was increased to improve the accuracy of parameter updating. Experiments show that the data-driven control method can optimize online to calculate the best control parameters and obtain the best control effect. It is found that the data-driven PID control can always complete the control task faster and more stable when the system changes control, better robustness, and response speed.

4 Conclusion

In thisarticle, the application of PID controller based on nonlinear system theory model free was studied. The main research is the algorithm of self-optimizing update of PID parameters. Online identification of solid oxide fuel cell (SOFC) voltage output dynamic model is realized by using radial basis function neural network under the condition that SOFC cannot obtain accurate analytical model; Jacobian information of voltage control model is obtained from the identified model to realize online adjustment of SOFC controller parameters. Because fuel utilization and control input constraints are the important factors to be considered in SOFC voltage control system, after the controller is designed, an anti-saturation compensator is connected in series, which is used to calculate the size of the reference object caused by the saturation effect, so as to ensure that the control signal is kept within the constraint range, the introduction of anti-saturation module also ensures that the error of parameter estimation is bounded rather than divergent. Theoretical analysis and simulation results show that it is effective and the control performance is better than the conventional PID control.

This study describes and analyzes the lazy learning algorithm and presents a PID control algorithm based on the improved lazy learning. The algorithm only needs to acquire the corresponding number of system input and output and then uses lazy learning to approximate the system model locally and update the model with the change of working point. After the estimation model is obtained, Jacobian information of the estimation model can be used to replace the corresponding information of the original system, and the adaptive updating law of PID parameters can be obtained by using the optimization algorithm. Finally, a simulation example is given to verify the effectiveness of the proposed method.

Funding information: This work was supported by Cooperative Project of Jiangsu Province production, teaching and research (No. BY2021381) and Jin Ling Institute of Technology Ph.D. Startup Fund (jit-b-202314).

Author contributions: This paper was written by Hongcheng Zhou.

Conflict of interest: I declare that I have no known competing financial interests or personal relationships that could have appeared to influence the work reported in this study.

Data availability statement: The data used to support the findings of this study are available from the corresponding author upon request.

References

[1] Wang, Y, Zhu K, Chen B, Jin M. Model-free continuous nonsingular fast terminal sliding mode control for cable-driven manipulators. ISA Trans. 2020;98:483–95. doi: 10.1016/j.isatra.2019.08.046.
[2] Roy S, Lee J, Baldi S. A new adaptive-robust design for time delay control under state-dependent stability condition. IEEE Trans Control Syst Technol. 2020;29(1):420–7. doi: 10.1109/TCST.2020.2969129.
[3] Wang Y, Yan F, Chen J, Ju F, Chen B. A new adaptive time-delay control scheme for cable-driven manipulators. IEEE Trans Ind Inform. 2019;15(6):3469–81. doi: 10.1109/TII.2018.2876605.
[4] Wu XQ, Xu KX, Zhang YB. Output-based feedback control of underactuated TORA systems by bounded inputs. Acta Autom Sin. 2020;46(1):200–4.
[5] Roman RC, Precup RE, Petriu EM, Dragan F. Combination of data-driven active disturbance rejection and Takagi-Sugeno fuzzy control with experimental validation on tower crane systems. Energies. 2019;12(8):1–19. doi: 10.3390/en12081548.
[6] Feng H, Song QY, Ma SL, Ma W, Yin CB, Cao DH, et al. A new adaptive sliding mode controller based on the RBF neural network for an electro-hydraulic servo system. ISA Trans. 2022;129:472–84. doi: 10.1016/j.isatra.2021.12.044.
[7] Aguilar-Ibanez C, Suarez-Castanon MS. A trajectory planning based controller to regulate an uncertain 3D overhead crane system. Int J Appl Math Comput Sci. 2019;29(4):693–702. doi: 10.2478/amcs-2019-0051.
[8] Zhang B, Cao R, Hou Z. The model-free adaptive cross-coupled control for two-dimensional linear motor. Trans Inst Meas Control. 2020;42(5):1059–69. doi: 10.1177/0142331219881830.
[9] Duan L, Hou ZS, Yu X, Jin ST, Lu KF. Data-driven model-free adaptive attitude control approach for launch vehicle with virtual reference feedback parameters tuning method. IEEE Access. 2019;7:54106–16. doi: 10.1109/ACCESS.2019.2912902.
[10] Abbaker O, Wang HP, Tian Y. Robust model-free adaptive interval type-2 fuzzy sliding mode control for PEMFC system using disturbance observer. Int J Fuzzy Syst. 2022;22:2188–203. doi: 10.1007/s40815-020-00916-8.
[11] Hou ZS, Xiong SS. On model-free adaptive control and its stability analysis. IEEE Trans Autom Control. 2019;64(11):4555–69. doi: 10.1109/TAC.2019.2894586.
[12] Borup KT, Stovner BN, Fossen TI, Johansen TA. Kalman filters for air data system bias correction for a fixed-wing UAV. IEEE Trans Control Syst Technol. 2019;28(6):2164–76. doi: 10.1109/TCST.2019.2931672.
[13] Qi G, Huang D. Modeling and dynamical analysis of a small-scale unmanned helicopter. Nonlinear Dyn. 2019;98:2131–45. doi: 10.1007/s11071-019-05313-x.
[14] Hg A, Me A, Hk B. Adaptive super-twisting non-singular terminal sliding mode control for tracking of quadrotor with bounded disturbances. Aerosp Sci Technol. 2021;112(1):106616. doi: 10.1016/j.ast.2021.106616.
[15] Qi G, Li X, Chen Z. Problems of extended state observer and proposal of compensation function observer for unknown model and application in UAV. IEEE Trans Syst Man Cybern Syst. 2022;52(5):2899–910. doi: 10.1109/TSMC.2021.3054790.
[16] Roy S, Kar IN. Adaptive sliding mode control of a class of nonlinear systems with artificial delay. J Frankl Inst. 2017;354(18):8156–79. doi: 10.1016/j.jfranklin.2017.10.010.
[17] Zhang X, Liu JG, Feng JK, Liu YW, Ju ZJ. Effective capture of nongraspable objects for space robots using geometric cage pairs. IEEE/ASME Trans Mechatron. 2020;25(1):95–107. doi: 10.1109/TMECH.2019.2952552.
[18] Zhang X, Liu JG. Effective motion planning strategy for space robot capturing targets under consideration of the berth position. Acta Astronaut. 2018;148:403–16. doi: 10.1016/j.actaastro.2018.04.029.
[19] Antonello A, Valverde A, Tsiotras P. Dynamics and control of spacecraft manipulators with thrusters and momentum exchange devices. J Guid Control Dyn. 2019;42(1):15–29. doi: 10.2514/1.G003601.
[20] Zhang X, Liu JG, Gao Q, Ju Z. Adaptive robust decoupling control of multi-arm space robots using time-delay estimation technique. Nonlinear Dyn. 2020;100(3):2449–67. doi: 10.1007/s11071-020-05615-5.